Revealing the Nature of Antiferroquadrupolar Ordering in Cerium Hexaboride: CeB$_6$

C. K. Barman,[1,*] Prashant Singh,[2,†] Duane D. Johnson,[2,3,‡] and Aftab Alam[1,§]

[1]*Department of Physics, Indian Institute of Technology, Bombay, Powai, Mumbai 400 076, India*
[2]*Ames Laboratory, U.S. Department of Energy, Ames, Iowa 50011, USA*
[3]*Materials Science & Engineering, Iowa State University, Ames, Iowa 50011, USA*

The cerium hexaboride (CeB$_6$) f-electron compound displays a rich array of low-temperature magnetic phenomena, including a "magnetically hidden" order, identified as multipolar in origin via advanced x-ray scattering. From first-principles electronic-structure results, we find that the *antiferroquadrupolar* (AFQ) ordering in CeB$_6$ arises from crystal-field splitting and yields a band structure in agreement with experiments. With interactions of p electrons between Ce and B$_6$ being small, the electronic state of CeB$_6$ is suitably described as Ce$(4f^1)^{3+}(e^-)(B_6)^{2-}$. The AFQ state of orbital spins is caused by an exchange interaction induced through spin-orbit interaction, which also splits the $J = 5/2$ state into a Γ_8 ground state and a Γ_7 excited state. Within the smallest antiferromagnetic (AFM) (111) configuration, an orbital-ordered AFQ state appears during charge self-consistency, and it supports the appearance of a "hidden" order. Hydrostatic pressure (either applied or chemically induced) stabilizes the AFM (AFQ) states over a ferromagnetic one, as observed at low temperatures.

The nature and first-principles description of f-electron materials is a considerable challenge and a highly debated topic in condensed-matter physics. The simultaneous presence of itinerant s-p-d states and partially occupied localized f states, and their interaction in rare-earth materials, gives rise to a rich variety of phenomena, and this remains a serious test for electronic-structure theories [1]. Rare-earth compounds with $4f$ electrons possessing orbital plus spin degrees of freedom generally show electric quadrupole ordering in addition to magnetic dipole ordering at low temperatures [2,3]. In Cerium-based compounds, the single $4f$ electron gives rise to anomalous and fascinating behavior, such as heavy-fermion, intermediate valence compounds, Kondo metals, and Kondo insulators [4–8].

Cerium hexaboride (CeB$_6$) is considered as a typical example of an f-electron system, where Ce^{+3} ions are arranged in the simple cubic lattice and quadrupolar interactions play an important role in its magnetic behavior [9,10]. It shows a unique antiferroquadrupolar (AFQ) ordering [5,11] at temperature $T_Q < 3.2$ K, associated with ordering of magnetic quadrupolar moments at cube corners [12,13]. Quadrupolar ordering is orbital in nature, arising due to the distortion of electronic charge density of the unpaired electrons in their $4f$ orbitals. The AFQ ordering has also been observed in compounds like DyB$_2$C$_2$, HoB$_2$C$_2$, TmTe, and PrOs$_4$Sb$_{12}$ [3,14–17].

The ordering phenomena in CeB$_6$ is acknowledged to be governed by antiferromagnetic (AFM) [18,19] interactions between multipolar moments of Ce-$4f$ electrons mediated by itinerant conduction electrons, which lift the degeneracy of the Γ_8 state of the Ce ions in their cubic crystal field [4,20]. Although the energy of the $4f$ electron is in the range of $5d$ and $6s$ valence electrons, its wave function is spatially localized and tighter than semicore $5s$ and $5p$ electrons. The competition between the Ce $4f$ electron being itinerant or localized determines the character of the compounds. The challenge is to describe coexistent near-degenerate, low-temperature phases [21–24] that arise from Ce-$4f$ hybridization with B conduction electrons. Jang, *et al.* [13] highlighted the ferromagnetic (FM) correlations in CeB$_6$ and suggested an intimate interplay between orbital [25–27] and magnetic ordering [18,19].

To investigate AFM (magnetic) and AFQ (charge) ordering, we explore the electronic structure using first-principles density functional theory (DFT) with increased orbital (charge) and magnetic degrees of freedom, and we find close agreement with the experiments [28]. Using a $2 \times 2 \times 2$ supercell with inequivalent Ce atoms, we use DFT as implemented in the Vienna *ab initio* simulation package (VASP) [29,30] to permit different charge and magnetic periodicities. The valence interactions were described by a projector augmented-wave method [30,31] with an energy cutoff of 320 eV for the plane-wave orbitals. We use $7 \times 7 \times 7$ Monkhorst-Pack k mesh for Brillouin zone sampling [32]. The total energies were converged to 10^{-5} eV/cell. We employ the Perdew-Bueke-Ernzerhof (PBE) [33] exchange-correlation functional in the generalized gradient approximation (GGA). In (semi)local functionals, such as GGA, the f electrons are always delocalized due to their large self-interaction error. To enforce the localization of the f electrons, we perform PBE + U calculations [34] with a Hubbard U (3 eV; $J = 1$ eV) introduced in a screened

Hartree-Fock manner [35]. See the Supplemental Material for more on choices of U, which includes Refs. [36–40]. The relativistic spin-orbit coupling (SOC) is also included, and it provides an interaction between the atomic orbital angular momentum and electron spin, which is a small perturbation of electrons in solids except for heavy elements with f orbitals, where it need not be weak—it effectively increases proportionally to Z^4 (Z is the atomic number).

Crystal structure and valency.—CeB$_6$ possesses a unique simple-cubic structure (space group $Pm\bar{3}m$) comprised of Ce^{3+} ions separated by B$_6$ octahedra, see Fig. 1(a), with the lattice constant a of 4.14 Å [41]. The calculated lattice constant of 4.147 Å shows a good agreement with experiments [41]. The structure can be considered as two interpenetrating simple-cubic sublattices, with one consisting of B$_6$ octahedra and the other of Ce ions. Notably, B$_6$ octahedra, which form a covalently bonded structure, require two additional electrons from the Ce ions to be stabilized [42,43]. The Ce valence is [Xe]$4f^1 5d^1 6s^2$, with the two s electrons being donated to the B$_6$ octahedra, and it is generally considered that the f-electron states remain localized with the d electrons forming the conduction band, resulting in the Ce^{3+} ion. Grushko *et al.* compared the x-ray chemical shift with the self-consistent Dirac-Fock-Slater-Latter calculation, and they concluded that the trivalent rare-earth atoms in hexaboride with metallic conduction donate two electrons to the boron framework, and that a third valence electron exists in the 5d orbitals. [42].

Initially Ce^{3+} multiplet $4f^1$ was thought to be split by the crystalline electric field into a Γ_7 ground state with a Γ_8 excited state [44]. However, this was later reversed to the Γ_8 quartet ground state, which is fourfold degenerate with 2-orbital and 2-spin degrees of freedom, located 46 meV below the Γ_7 doublet state [23,45,46]. Our present results give ∼62 meV separation between Γ_7 and Γ_8, reflecting experimentally findings. The Raman scattering measurements provide an explanation for these observations, indicating that the Γ_8 quartet is further split into two doublets, $\Gamma_{8,1}$ and $\Gamma_{8,2}$, separated by around 30 K [45].

In Fig. 1(c), we show the band structure and density of states (DOS) for FM states. The low-T phase and its electronic structure are mainly governed by the dispersive 5d and flat 4f bands, shown along M-X-M and X-Γ-X. The flat bands near the Fermi energy (E_{Fermi}) arise purely from Ce-4f states. The dispersive d band (X points) is found to be about −2.0 eV below E_{Fermi} and the dispersive B 2p bands are near the bottom of this d band. These bands at or near the X point agree fairly well with experiments [28,47]. One immediately notices the location of flat Ce-4f bands slightly below E_{Fermi}, as observed in ARPES data [28], although their energy positions differ slightly. DOS show similar behavior, but with most significant density below E_{Fermi}. Importantly, a parabolic band along X-Γ-X forms close to E_{Fermi} at Γ giving a holelike pocket, as observed in Refs. [28,47]. A strong renormalization of bands near
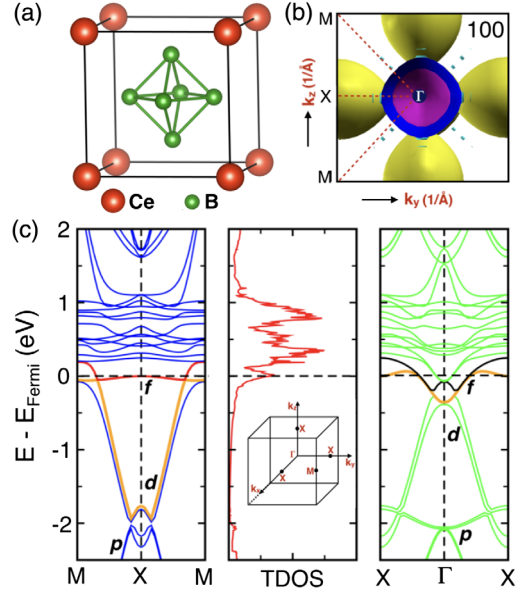

FIG. 1. For FM CeB$_6$, (a) $Pm\bar{3}m$ crystal structure, (b) (100) Fermi surface, and (c) bands (with SOC) along M-X-M and X-Γ-X, with p, d, and f states identified, and density of states (DOS). Inset: Brillouin zone and high-symmetry points.

E_{Fermi} at the Γ point occurs in both of these cases. Several features in these bands can be corroborated with the ARPES data [28,47]. Parabolic shaped bands near E_{Fermi} at the Γ point which are relatively more flat compared to those in ARPES data [28,47]. In contrast to previous calculations [28,47], we find a holelike character near at Γ. The calculated Fermi surface, Fig. 1(b), is in good agreement with observations [28,47], i.e., hole pockets, including an oval-shaped contour at X, are found. The spectral intensities around Γ are stronger compared to those at X. The two Fermi-surface contours [blue and magenta around Γ in Fig. 1(b)] represent the band splitting. In Fig. 1(b), the holelike pocket at Γ, with strongly renormalized bands, corresponds to the observed, so-called *hot spots* [28,47]. The emergence of a low-temperature magnetic order is highly possible if these states are extremely close in energy relative to the FM case.

CeB$_6$ has been investigated intensively at low temperature due to its unusual properties such as AFQ ordering, the Kondo effect (which makes the localized Ce moment vanish due to coupling of Ce and B moments), and the Ruderman-Küttel-Kasuya-Yoshida (RKKY) interaction (which arranges the moments of the AFM Ce with the moments of itinerant electrons of B) [48,49]. These properties are closely connected with the localized $4f(\Gamma_8)$ electrons of Ce and conduction electrons of B. Including SOC interactions resolves most of the differences except the presence of AFQ-type charge ordering. To elucidate on the AFQ phase, we perform a similar SOC + U calculation on a larger supercell with an AFM arrangement of spins on Ce1 [along (111)] and Ce2 [along -(111)] see Fig. 2(b).
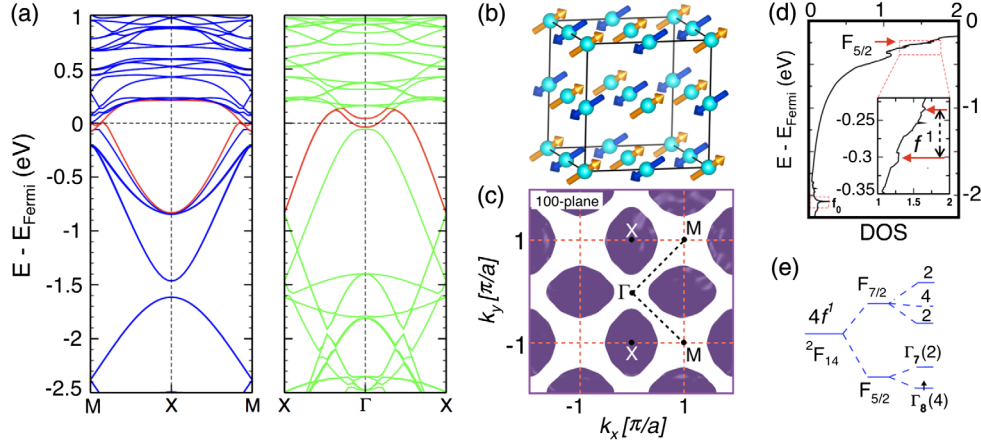
FIG. 2. For AFM CeB_6, (a) DFT + U dispersion along M-X-M and X-Γ-X. (b) Schematic of AFM state. (c) (100) constant energy surface plot at -0.30 eV below Fermi-energy (Γ_7 and Γ_8 splitting is observed in -0.20 to -0.35 eV energy range). (d) Ce$-f$ DOS (matches experiment) [28]. (e) Energy-level diagram with SOC and crystal-field splitting.

From the band structure of CeB_6, Fig. 2(a), the $4f$ bands are hybridized with the $5d$ band around E_{Fermi} [50] of CeB_6. The $4f$ bands are centered at the X point in the Brillouin Zone, which is the center of the B—B bond and has hybridized character of Ce-$5d$ and B-$2p$ states [51,52]. The calculated constant energy surface plot in Fig. 2(c) at -0.30 eV below E_{Fermi} consists of ellipsoids centered about the X point, and are typical for the hexaborides [28,47], in agreement with previous measurements [28,47,51,53]. Their ellipsoid orbital character is composed of extended Ce-$5d$ states with admixtures of localized Ce-$4f$ near E_{Fermi}, similar to other $4f$ systems exhibiting a resonance mode [54,55]. The large electronlike constant energy surface plot centered at X (M) point is in good agreement with experiments [51,52]. The ellipsoidal-shape in the constant energy surface plot, elongated along the $X(M)$-$\Gamma(X)$, does support the assumptions of the two models used to explain the AFQ and AFM ordering in CeB_6 [56,57].

The valence-band structure along the M-X-M and the X-Γ-X direction is shown in Fig. 2(a) in the cubic Brillouin zone [52]. We find that the gross feature of band structure is in good agreement with existing experiments. According to the band calculation, the observed dispersive bands in this energy range are attributed to the bonding B $2s-2p$ state of the octahedron. Also, the nondispersive band at 2.1 eV belongs to Ce-d states. The band along X-Γ-X direction has a parabolic (or U) shape, whereas the bottom of the band appears more cusplike (or V shaped) along M-X-M. Near E_{Fermi}, the screened f^1 states are found, which split due to the spin-orbit coupling in a J equals $5/2$ and $7/2$ component. The $5/2$ state at E_{Fermi} is relevant here and splits further into crystal-field levels under SOC and DFT + U, see Fig. 2, namely, a Γ_7 doublet (excited state) and a Γ_8 quartet [58]. One of the Γ_8 levels is occupied, whereas the Γ_7 intensity seen in the spectrum is a satellite. The energy separation of the Γ_7 and Γ_8 levels (62 meV) is

in agreement with previous reports [59,60]. Note that the large ground-state degeneracy distinguishes CeB_6 from many other Ce-based heavy-fermion materials.

The $4f$ state in Ce ions with a stable valency has the orbital freedom in addition to the spin. The ground state multiplet due to the spin-orbit interaction splits into the crystalline electric field state by the multipolar Coulomb potential. As shown in the level splitting in the f^1 configuration, Γ_8 is lower than Γ_7. In Fig. 2(d), the localized f^0 ionization peak of Ce-f at -2.05 eV overlaps with the bottom of the ellipsoid band, and it agrees with those of the integrated energy distribution from experiments [28,47]. Below E_{Fermi}, the screened f^1 states of Ce, located between -0.2 to -0.35 eV, splits into J $5/2$ and $7/2$ components due to SOC. Interestingly, the $4f(j = 5/2)$ orbital further splits into Γ_7 (doublet) excited states and Γ_8 (quartet) ground states under O_h crystal field. To emphasize, for Γ_8 to be ground state, the SOC interaction should be larger than the Hund's rule interaction [61,62]. As such, the energy level of the $4f(5/2)$ orbitals remains lower than the $4f(7/2)$ orbitals. Ce^{3+} formally has one $4f$ electron. The Γ_7 and Γ_8 differ in energy by 62 meV, agreeing fairly well with the 50 meV from photoemission [28,47].

The schematic energy levels are illustrated in Fig. 2(e) [63]. In spite of the same local crystal-field anisotropy in AFM CeB_6, the opposite moments on Ce1 and Ce2 result in no gain in energy due to the magnetic dipole interaction. This unusual magnetic structure is now understood to be a consequence of the underlying AFQ order, which confines the direction of the magnetic moment by a strong spin-orbit coupling.

In AFQ CeB_6, the $4f$ electrons are localized, having an orbitally degenerate level in the crystalline electric-field ground state. As shown in Fig. 3, the orbital ordering in f-electron systems, i.e., a spontaneous lifting of the orbital degeneracy, is a phase transition of quadrupole moments.
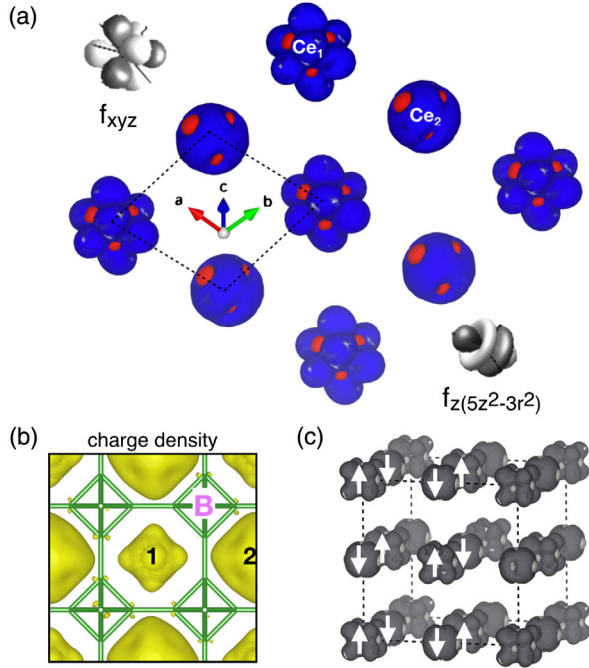
FIG. 3. For AFM CeB_6, we show (a) (111)-projected Ce1 (f_{xyz}) and Ce2 ($f_{z(5z^2-3r^2)}$) orbitals, (b) total charge density in (001) plane, and (c) schematic of AFM Ce configuration. Together these show distinct AFM and orbital arrangement at the Ce1 and Ce2 sites, indicating the underlying AFQ order.

The orbital degeneracy is then described in terms of quadrupole moments due to the presence of strong intra-atomic SOC. Following the AFM ordering, one refers to the uniform alignment of the quadrupole moment, where this staggered quadrupolar component is called an AFQ state. The effect is also visible in Fig. 3(b) through contrasting charge density at the Ce1 and Ce2 sites. For CeB_6, an AFM state with an AFQ background is evident in Fig. 3(c).

From the axial interaction with B-p states, the Ce-f states (f_{xyz} and $f_{z(5z^2-3r^2)}$) are modified and produce a weak electric quadrupolar ordering with (nearly) degenerate localized states. The charge distributions on Ce1 and Ce2, in Fig. 3(b), comes from f_{xyz} and $f_{z(5z^2-3r^2)}$ orbitals, respectively, giving a distinct shape to the charge density. This underlying ("hidden") AFQ ordering is difficult to observe as this arises mainly from a weaker quadrupolar interaction and the electron density in the given unit cell spontaneously distorts in a repeating pattern throughout the crystal.

For any admixture of magnetic-dipole, charge-order, or sufficiently large lattice distortion, the neutron scattering shows indirect coupling to the multipolar order but remains unchanged in the quadrupolar AFQ phase [64]. URu_2Si_2 is one such example [65]. In Fig. 4, we show the effect of (hydrostatic) pressure on the relative energy of FM and AFM states, where they are degenerate near 21 GPa (−2.5% change in lattice constant), above which the AFM is stable. The simulated energy difference between
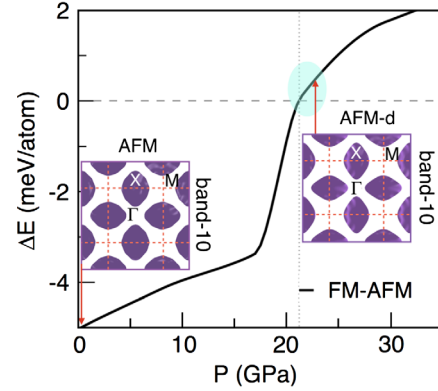

FIG. 4. For CeB_6, FM-AFM energy difference vs pressure, which alters hybridization between $4f$ bands and dispersive $5d$ bands (Inset: AFM constant energy surface (hole states) at −0.30 eV below E_{Fermi} at 0 and 21 GPa. Holelike states appear at Γ and X points (see Fig. S8) [28].

the FM and AFM phases lies within a few meV (1 meV is equivalent to 11 Kelvin). Such small energy difference sometimes acts as the precursor for magnetic phase instability and infers the co-existence of magnetic domains. This point is carefully taken up in a recent study using high intensity inelastic neutron scattering [13]. The competition between FM and AFM states is sensitive to pressure due to the hybridization between flat $4f$ bands and low-lying dispersive $5d$ bands, as reflected in the constant energy surface plot changes in shape and size of the hole pockets at the X point (Fig. 4). However, the pattern is similar to those observed by Neupane *et al.* [28], and it clearly shows the presence of holelike states (X point).

In summary, we have provided direct electronic insight to the presence of antiferroquadrupolar ordering in CeB_6. The crystal-field splitting, controlled by spin-orbit coupling, yields electronic dispersion and a constant energy surface below E_{Fermi} (electron and hole pockets) that agrees fairly well with those observed from ARPES, highlighting the importance of spin-orbit coupling in f-block systems. Furthermore, our calculations reveal that the dispersion around Γ is strongly renormalized, as indicated by highly increased density of states there, which are observed as hot spots in ARPES. The competition between FM and AFM states is sensitive to pressure (both applied and chemically induced), which alters the hybridization between flat $4f$ bands and low-lying dispersive $5d$ bands. Finally, with a recent finding of the topologically insulated phase in SmB_6, the search for a topological insulator phase with magnetically active sites in CeB_6 may be warranted.

* chanchal_barman@iitb.ac.in
† Corresponding author.
  prashant40179@gmail.com
‡ ddj@iastate.edu
§ aftab@phy.iitb.ac.in

[1] M. Casadei, X. Ren, P. Rinke, A. Rubio, and M. Scheffler, Phys. Rev. Lett. **109**, 146402 (2012).

[2] T. Yanagisawa, T. Goto, Y. Nemoto, R. Watanuki, K. Suzuki, O. Suzuki, and G. Kido, Phys. Rev. B **71**, 104416 (2005).

[3] H. Yamauchi, T. Osakabe, E. Matsuoka, and H. Onodera, J. Phys. Soc. Jpn. **81**, 034715 (2012).

[4] R. Shiina, H. Shiba, and P. Thalmeier, J. Phys. Soc. Jpn. **66**, 1741 (1997).

[5] Y. Kuramoto, H. Kusunose, and A. Kiss, J. Phys. Soc. Jpn. **78**, 072001 (2009).

[6] R. Shiina, O. Sakai, H. Shiba, and P. Thalmeier, J. Phys. Soc. Jpn. **67**, 941 (1998).

[7] H. Shiba, O. Sakai, and R. Shiina, J. Phys. Soc. Jpn. **68**, 1988 (1999).

[8] G. Friemel, Y. Li, A. V. Dukhnenko, N. Y. Shitsevalova, N. E. Sluchanko, A. Ivanov, V. B. Filipov, B. Keimer, and D. S. Inosov, Nat. Commun. **3**, 830 (2012).

[9] D. Hall, Z. Fisk, and R. G. Goodrich, Phys. Rev. B **62**, 84 (2000).

[10] S. W. Lovesey, J. Phys. Condens. Matter **14**, 4415 (2002).

[11] P. Santini, S. Carretta, G. Amoretti, R. Caciuffo, N. Magnani, and G. H. Lander, Rev. Mod. Phys. **81**, 807 (2009).

[12] M. Sera, H. Ichikawa, T. Yokoo, J. Akimitsu, M. Nishi, K. Kakurai, and S. Kunii, Phys. Rev. Lett. **86**, 1578 (2001).

[13] H. Jang, G. Friemel, J. Ollivier, A. V. Dukhnenko, N. Yu. Shitsevalova, V. B. Filipov, B. Keimer, and D. S. Inosov, Nat. Mater. **13**, 682 (2014).

[14] K. Hirota, N. Oumi, T. Matsumura, H. Nakao, Y. Wakabayashi, Y. Murakami, and Y. Endoh, Phys. Rev. Lett. **84**, 2706 (2000).

[15] Y. Tanaka, T. Inami, T. Nakamura, H. Yamauchi, H. Onodera, K. Ohoyama, and Y. Yamaguchi, J. Phys. Condens. Matter **11**, L505 (1999).

[16] J.-M. Mignot, P. Link, A. Gukasov, T. Matsumura, and T. Suzuki, Physica (Amsterdam) **281B–282B**, 470 (2000).

[17] R. Shiina, J. Phys. Soc. Jpn. **75**, 114708 (2006).

[18] A. Steppke, R. Küchler, S. Lausberg, E. Lengyel, L. Steinke, R. Borth, T. Lühmann, C. Krellner, M. Nicklas, C. Geibel, F. Steglich, and M. Brando, Science **339**, 933 (2013).

[19] O. Zaharko, P. Fischer, A. Schenck, S. Kunii, P. J. Brown, F. Tasset, and T. Hansen, Phys. Rev. B **68**, 214401 (2003).

[20] P. Thalmeier, R. Shiina, H. Shiba, A. Takahashi, and O. Sakai, J. Phys. Soc. Jpn. **72**, 3219 (2003).

[21] P. Thalmeier, R. Shiina, and O. Sakai, J. Phys. Soc. Jpn. **67**, 2363 (1998).

[22] H. Shiba, O. Sakai, and R. Shiina, J. Phys. Soc. Jpn. **68**, 1988 (1999).

[23] N. Sato, S. Kunii, I. Oguro, T. Komatsubara, and T. Kasuya, J. Phys. Soc. Jpn. **53**, 3967 (1984).

[24] J. M. Effantin, Ph. D. thesis, Universit Scientifique et Medical de Grenoble, 1985.

[25] H. Nakao, K.-I. Magishi, Y. Wakabayashi, Y. Murakami, K. Koyama, K. Hirota, Y. Endoh, and S. Kunii, J. Phys. Soc. Jpn. **70**, 1857 (2001).

[26] T. Matsumura, T. Yonemura, K. Kunimori, M. Sera, and F. Iga, Phys. Rev. Lett. **103**, 017203 (2009).

[27] T. Matsumura, T. Yonemura, K. Kunimori, M. Sera, F. Iga, T. Nagao, and J.-I. Igarashi, Phys. Rev. B **85**, 174417 (2012).

[28] M. Neupane *et al.*, Phys. Rev. B **92**, 104420 (2015).

[29] G. Kresse and J. Hafner, Phys. Rev. B **47**, 558 (1993).

[30] G. Kresse and D. Joubert, Phys. Rev. B **59**, 1758 (1999).

[31] P. E. Blöchl, Phys. Rev. B **50**, 17953 (1994).

[32] H. J. Monkhorst and J. D. Pack, Phys. Rev. B **13**, 5188 (1976).

[33] J. P. Perdew, K. Burke, and M. Ernzerhof, Phys. Rev. Lett. **77**, 3865 (1996).

[34] S. L. Dudarev, G. A. Botton, S. Y. Savrasov, C. J. Humphreys, and A. P. Sutton, Phys. Rev. B **57**, 1505 (1998).

[35] M. Tang, L. Liu, Y. Cheng, and G.-F. Ji, Front. Phys. **10**, 107104 (2015); H. Lu and Li Huang, Phys. Rev. B **95**, 155140 (2017).

[36] C. Loschen, J. Carrasco, K. M. Neyman, and F. Illas, Phys. Rev. B **75**, 035115 (2007).

[37] S. Fabris, S. de Gironcoli, S. Baroni, G. Vicario, and G. Balducci, Phys. Rev. B **71**, 041102(R) (2005).

[38] J. L. F. Da Silva, Phys. Rev. B **76**, 193108 (2007).

[39] D. A. Andersson, S. I. Simak, B. Johansson, I. A. Abrikosov, and N. V. Skorodumova, Phys. Rev. B **75**, 035109 (2007).

[40] See Supplemental Material at http://link.aps.org/supplemental/10.1103/PhysRevLett.122.076401 for further supporting results related to discussion in the main text, such as structural property, choice of U, electronic-structure and Fermi-surface for CeB_6.

[41] L. Liu, Y.-M. Yiu, and T.-K. Sham, J. Electron Spectrosc. Relat. Phenom. **184**, 188 (2011).

[42] Y. S. Grushko, Y. B. Paderno, K. YaMishin, L. I. Molkanov, G. A. Shadrina, E. S. Konovalova, and E. M. Dudnik, Phys. Status Solidi B **128**, 591 (1985).

[43] H. C. Languet-Higgins and M. de V. Roberts, Proc. R. Soc. A **224**, 336 (1954).

[44] J. C. Nickerson and R. M. White, J. Appl. Phys. **40**, 1011 (1969).

[45] E. Zirngiebl, B. Hillebrands, S. Blumenroder, G. Güntherodt, M. Loewenhaupt, J. M. Carpenter, K. Winzer, and Z. Fisk, Phys. Rev. B **30**, 4052 (1984).

[46] M. Loewenhaupt, J. Carpenter, and C. K. Loong, J. Magn. Magn. Mater. **52**, 245 (1985).

[47] A. Koitzsch, N. Heming, M. Knupfer, B. Büchner, P. Y. Portnichenko, A. V. Dukhnenko, N. Y. Shitsevalova, V. B. Filipov, L. L. Lev, V. N. Strocov, J. Ollivier, and D. S. Inosov, Nat. Commun. **7**, 10876 (2016).

[48] N. Sato, A. Sumiyama, S. Kunii, H. Nagano, and T. Kasuya, J. Phys. Soc. Jpn. **54**, 1923 (1985).

[49] O. Sakai, R. Shiina, H. Shiba, and P. Thalmeier, J. Phys. Soc. Jpn. **66**, 3005 (1997).

[50] P. V. D. Heide, H. W. T. Cate, L. M. T. Dam, R. A. D. Groot, and A. R. D. Vroomen, J. Phys. F **16**, 1617 (1986).

[51] S. Souma, Y. Iida, T. Sato, T. Takahashi, and S.Kunii, Physica (Amsterdam) **351B**, 283 (2004).

[52] H. Harima, O. Sakai, T. Kasuya, and A. Yanase, Solid State Commun. **66**, 603 (1988).

[53] Y. Onuki, T. Komatsubara, P. H. P. Rein-ders, and M. Springford, J. Phys. Soc. Jpn. **58**, 3698 (1989).

[54] C. Stock, C. Broholm, J. Hudis, H. J. Kang, and C. Petrovic, Phys. Rev. Lett. **100**, 087001 (2008).

[55] A. Koitzsch, T. K. Kim, U. Treske, M. Knupfer, B. Büchner, M. Richter, I. Opahle, R. Follath, E. D. Bauer, and J. L. Sarrao, Phys. Rev. B **88**, 035124 (2013).

[56] Y. Kurmamoto and K. Kuboy, J. Phys. Soc. Jpn. **71**, 2633 (2002).

[57] P. Schlottmann, Phys. Rev. B **62**, 10067 (2000).

[58] W. Knafo, S. Raymond, B. Fak, G. Lapertot, P. C. Canfield, and J. Flouquet, J. Phys. Condens. Matter **15**, 3741 (2003).

[59] E. Zirngiebl, B. Hillebrands, S. Blumenröder, G. Güntherodt, M. Loewenhaupt, J. M. Carpenter, K. Winzer, and Z. Fisk, Phys. Rev. B **30**, 4052 (1984).

[60] T. Takahashi, T. Morimoto, T. Yokoya, S. Kunii, T. Komatsubara, and O. Sakai, Phys. Rev. B **52**, 9140 (1995).

[61] M. Loewenhaupt and M. Prager, Z. Phys. B **62**, 195 (1986).

[62] S. Kobayashi, M. Sera, M. Hiroi, T. Nishizaki, N. Kobayashi, and S. Kunii, J. Phys. Soc. Jpn. **70**, 1721 (2001).

[63] R. Makita, K. Tanaka, and Y. Ōnukib, Acta Crystallogr. Sect. B **64**, 534 (2008).

[64] H. Yamauchi, H. Onodera, K. Ohoyama, T. Onimaru, M. Kosaka, M. Ohashi, and Y. Yamaguchi, J. Phys. Soc. Jpn. **68**, 2057 (1999).

[65] J. A. Mydosh and P. M. Oppeneer, Rev. Mod. Phys. **83**, 1301 (2011).